

Marcus Wilms · Simon B. Eickhoff · Karsten Specht
Katrin Amunts · Nadim J. Shah
Aleksandar Malikovic · Gereon R. Fink

Human *V5/MT+*: comparison of functional and cytoarchitectonic data

Published online: 19 November 2005
© Springer-Verlag

Abstract To date, the delineation of the human visual “motion area” still relies on functional paradigms originally devised to identify monkey area *MT*. Using fMRI, we have identified putative human area *V5/MT+* in normals by modelling the BOLD responses to alternating radially moving and stationary dot patterns. Functional activations were compared with cytoarchitectonic probability maps of its putative correlate area *hOc5*, which was calculated based upon data from histological sections of ten human post-mortem brains. Bilateral visual cortex activations were seen in the single subject *dynamic versus stationary* contrasts and in the group random-effects analysis. Comparison of group data with area *hOc5* revealed that 19.0%/39.5% of the right/left functional activation was assigned to the right/left *hOc5*. Conversely, 83.2%/53.5% of the right/left *hOc5* was functionally activated. Comparison of functional probability maps (fPM) with area *hOc5* showed that 28.6%/18.1% of the fPM was assigned to *hOc5*. In turn, 84.9%/41.5% of the area *hOc5* was covered by the respective fPM. Thus, random-effects data and fPMs yielded sim-

ilar results. The present study shows for the first time the correspondence between the functionally defined human *V5/MT+* and the post-mortem cytoarchitectonic area *hOc5*.

Keywords Functional probability map · fMRI · Motion · Post-mortem · Visual cortex

Introduction

In the primate, a motion-sensitive area in the occipitotemporal visual cortex was the first to be identified both functionally and with respect to its anatomy (Zeki 1974). It was named area *V5* or area *MT*, after its middle temporal location in the owl monkey (Allman and Kaas 1971), and more recently area *MT+* indicating that it probably comprises functionally segregated subregions (Dukelow et al. 2001; Huk et al. 2002). In the macaque, it is now well accepted that the preference of *V5/MT+* for motion stimuli is rooted in the receptive field properties of retinal *M* ganglion cells, which project exclusively to neurons of the magnocellular subdivisions of the dorsal lateral geniculate nucleus (Zeki 1993). This magnocellular pathway has been shown to project to area *V5/MT+* (Maunsell et al. 1990). With the advent of non-invasive brain imaging tools like positron emission tomography (PET) (Watson et al. 1993) and functional magnetic resonance imaging (fMRI) (Tootell et al. 1995), human motion processing was investigated more directly. Both techniques confirmed the existence of a bilateral motion-sensitive area *V5/MT+* that may coincide with Flechsig’s *Feld 16* (Watson et al. 1993; Flechsig 1927).

Functional brain segregation is often assumed to ultimately rely on an anatomical basis, be it as obvious as in the striate appearance of the primary visual cortex or more hidden in distinct cytoarchitectonic differences between brain areas. For example, a close correspondence of functional and architectonic segregation has been shown for the primary visual areas *V1* and *V2*

M. Wilms (✉) · S. B. Eickhoff · K. Specht · K. Amunts
N. J. Shah · A. Malikovic · G. R. Fink
Institute of Medicine, Research Centre Jülich,
52425 Jülich, Germany
E-mail: ma.wilms@fz-juelich.de
Tel.: +49-2461-616184
Fax: +49-2461-611518

K. Amunts
Department of Psychiatry and Psychotherapy—Brain Mapping,
University Hospital Aachen, RWTH Aachen, Aachen, Germany

N. J. Shah · G. R. Fink
Brain Imaging Centre West, Research Centre Jülich,
Jülich, Germany

N. J. Shah
Institute of Physics, University of Dortmund,
Dortmund, Germany

G. R. Fink
Department of Neurology—Cognitive Neurology, University
Hospital Aachen, RWTH Aachen, Aachen, Germany

(Amunts et al. 2000; Wohlschläger et al. 2005). With regard to area $V5/MT+$, Malikovic et al. (2001) as well as Annese et al. (2005) reported a putative human correlate of $V5/MT+$ applying observer-independent analyses of cortical cytoarchitecture in human post-mortem brains. Based on cytoarchitectonic probabilistic maps of putative $V5/MT+$ (Malikovic et al. 2001) the present study investigates whether this area corresponds to its functionally defined counterpart.

For this purpose, the neural mechanisms underlying visual motion processing were located using fMRI in healthy volunteers. In one approach, functional single subject and random effects group activation maps were calculated from the functional *t*-statistic contrasts for *dynamic versus stationary* stimulation. In order to resemble the generation of the anatomical probability maps (aPM) more closely, functional probability maps (fPM) were also calculated from the single subject contrasts. Both, random effects group activation maps and fPMs were then quantitatively compared with the aPMs of putative human $V5/MT+$ obtained from post-mortem brains using a percent overlap measure, in order to test the hypothesis that functionally defined $V5/MT+$ and the anatomically defined equivalent overlap and hence correspond to each other.

Methods

Subjects

Fourteen healthy subjects aged 18–39 years (nine females and five males, 23 ± 5 years) participated in the functional imaging measurements. Functional data were collected from a mixed group of male and female volunteers to reflect the mixed set of post-mortem brains (five females, five males). All subjects were healthy and without any history of neurological or psychiatric diseases, had normal visual acuity, and were right-handed as assessed by the Edinburgh inventory (Oldfield 1971), with an average laterality quotient of 84%. Subjects gave informed written consent before participating in the study.

Visual stimuli

The stimuli for localizing area $V5/MT+$ were similar to those used in other fMRI studies (Tootell et al. 1995; Huk et al. 2002). Radially moving or stationary white dots ($n = 500$), each with a Gaussian spatial luminance profile (0.4° absolute width), covered a 17° circular grey aperture of a visual stimulation device (*goggles*, Silent VisionTM, Avotec, FL, USA). Stimulus sequences were custom programmed using IDL software (Version 6.0 (c) 2003, Research Systems Inc., Boulder, CO, USA). The stimulus presentation was controlled with the PresentationTM software (Version 0.76, <http://www.neurobs.com>). Moving dots travelled at $6.5^\circ/s$ and coherently

changed their movement direction every 1.3 s (radially inward and outward from a central fixation cross). Blocks of dynamic and stationary stimulation lasted for 18 s each. Eight pairs of dynamic-stationary blocks were presented in a row (~ 5 min) before the subject was allowed a short pause. This paradigm was repeated four times yielding a total of 20 min presentation time for the whole experiment. Subjects were asked to always fixate a high-contrast red fixation cross in the middle of their visual field. Despite the possibility of an enhanced signal-to-noise ratio (Beauchamp et al. 1997; O'Craven et al. 1997), no further attentional factors were included to minimise the contribution of confounds (Zeki et al. 1991). The subjects' eye movements were qualitatively monitored throughout the measurements by means of an infra-red camera (Avotec Real EyeTM, FL, USA).

Functional MRI

MRI was carried out using a 1.5 T scanner (Siemens Magnetom Sonata, Erlangen, Germany) with a standard head coil for radio-frequency transmission and signal reception. A whole brain T1-weighted anatomical MRI ($1 \times 1 \times 1 \text{ mm}^3$) was acquired for every subject using the 3D MP-RAGE sequence (Mugler and Brookeman 1990) with parameters: repetition time (TR) = 2.2 s, echo time (TE) = 3.93 ms, inversion time (TI) = 1.2 s, flip angle (FA) = 15° , field of view (FOV) = 256 mm.

Multislice T2*-weighted echoplanar images (EPI) were obtained from a gradient-echo sequence that employed the following pulse sequence parameters: TR = 3.15 s, TE = 66 ms, FA = 90° , FOV = $200 \times 200 \text{ mm}^2$, slice thickness = 4 mm, inter-slice gap = 0.4 mm, in-plane resolution = $3.125 \times 3.125 \text{ mm}^2$, matrix size = 64×64 . Thirty fMRI slices were oriented parallel to the calcarine sulcus and covered the whole brain. Head movements were minimised by the slight pressure of the protective headphones on either side of the head and the goggles' oculars on the eyebrows. The scanning procedure was performed continuously over the entire experiment including pauses (20 min).

Image processing

Most of the data analysis, including realignment, slice timing, normalisation, and statistical analysis of the EPI time series was performed using the SPM2 software (Wellcome Department of Imaging Neuroscience, London, UK, <http://www.fil.ion.ucl.ac.uk/spm>) implemented in MATLAB (Mathworks, Inc., Sherborn, MA, USA). The first three fMRI volumes were discarded to avoid transient magnetic saturation effects and to allow for the haemodynamic response to reach steady state. Images were realigned to compensate for the subjects' head movements during scanning. Slice acquisition timing was interpolated to the acquisition time of the middle slice. The 3D-anatomical data set was coregis-

tered to the mean EPI image and then spatially normalised to the stereotactic space defined by the single-subject template provided by the Montreal Neurological Institute (MNI) (Evans et al. 1992; Collins et al. 1994; Holmes et al. 1998). The normalisation parameters were then applied to the EPI volumes yielding all EPI data with $3 \times 3 \times 3 \text{ mm}^3$ voxel size in MNI space. This was crucial as we wanted to compare functional activations with anatomical maps that were also defined in MNI space. Data were subsequently spatially smoothed with an isotropic Gaussian kernel of 8 mm at full-width half-maximum to compensate for normal variations in brain size and gyral patterns.

Subject-specific low-frequency drifts in the BOLD-signal (blood oxygen level dependent) were removed by a high-pass filter with 1/128 Hz cut-off.

Statistical analysis

The data were then analysed by defining a model for each subject containing the expected BOLD signal at any voxel. Therefore, regressors for the different stimulus conditions were defined using boxcar reference vectors for dynamic, stationary, and pause conditions, each convolved with a canonical haemodynamic response function (HRF). In addition to that a set of regressors convolved with the time derivative of the canonical HRF were included. Also, the six parameters obtained from the realignment procedure (describing translations and rotations of the head) were added to the design matrix. The estimated model parameters for *dynamic* and *stationary* regressors were linearly contrasted and yielded a *t*-statistic (further transformed to a *Z*-statistic) for each and every voxel. These *t*-statistics constitute a subject-specific statistical parametric map. Significant activation was assessed initially on a voxel-by-voxel basis. Corrections for multiple comparisons over the whole brain were implemented by using family-wise error correction (Friston et al. 1996). Areas were considered as significantly activated only if they passed a threshold of $P_{\text{corr}} < 0.01$ and extended over ten or more voxels.

Single subject *t*-statistic contrasts for *dynamic versus stationary* stimulation were entered into a random-effects analysis comparing the mean activation to the variability in activations from subject to subject ($P_{\text{corr}} < 0.05$, no extent threshold). Thus, inference about significant activations could be generalised to the population from which the subjects were selected. Besides this exploratory approach using a whole-brain correction for multiple comparisons advantage was taken of the a priori knowledge about the expected location of area *V5/MT+* from other fMRI studies (Table 2, bottom row). The maximum Euclidean displacement of any centre of *V5/MT+* activation in the literature data from the mean location of the literature data set was 14 mm. Adding an extra millimetre for the estimated half-width of the underlying point spread of activation, a small-volume correction was performed for multiple compar-

isons within a sphere of 15 mm radius around the mean location of the respective *V5/MT+* centres reported in other functional imaging studies. Voxels that exceeded the small-volume corrected *P*-value ($P_{\text{corr}} < 0.05$) in the group random effects analysis and lay within the search volume were then compared with the anatomical data.

As a different approach for analysing significant activations on the group level, we propose to superimpose thresholded single-subject functional *t*-maps yielding functional probability maps (fPM). Single-subject functional *t*-maps were thresholded at $P_{\text{corr}} < 0.01$ (voxel extent threshold = 10) and all significant voxels set to unity, non-significant voxels to zero. Such “binarised” *t*-maps were then added over all subjects on a voxel-by-voxel basis. Stereotactic voxels that were significantly activated in many subjects were regarded as more likely to belong to a certain functionally segregated area compared with voxels that were activated in only few subjects. As 14 subjects were included in this analysis, the fPMs took values ranging from 0 to 14. The calculation of fPMs thus resembles the procedure used for the generation of anatomical PMs, and thereby, facilitates a comparison of both data modalities.

Anatomical probability maps

Observer-independent cytoarchitectonic mapping was performed on histological sections stained for cell bodies of ten human post-mortem brains (Schleicher et al. 1999). This technique revealed an area in occipito-temporal visual cortex, *hOc5*, which showed a broad layer III, a high cell density in layers II/III, and a low cell density in layer V (Malikovic et al. 2001). After 3D reconstruction and registration to the single-subject reference space, an aPM of area *hOc5* was calculated by superimposing the individual area *hOc5* maps. The aPM was then thresholded at 40%, since we found in other brain regions that this threshold reflects the border of an isolated area (i.e. an area, to which neighbouring areas have not been mapped, yet), such as area *hOc5* most precisely (Eickhoff et al. 2005). In addition to the map of area *hOc5*, aPMs of Brodman areas 17 and 18 were applied for topographical interpretation of functional activations (Amunts et al. 2000).

Comparison of functional and anatomical maps

Both the functional random-effects maps and the fPMs were resampled to the isotropic $1 \times 1 \times 1 \text{ mm}^3$ resolution of the aPMs. This facilitated the quantitative comparison of functional and anatomical maps using a custom-programmed MATLAB toolbox (*Anatomy v0.3*, Eickhoff et al. 2005). Like the aPMs, fPMs were thresholded at 40%. The amount of overlap is given as the percentage of the target area. For example, assume a functionally defined area is twice as large as its anatomically defined counterpart. If 40% of the functionally

defined volume lies within the anatomically defined counterpart, 80% of the anatomically defined region is activated. Thus percent-overlap values strongly depend on the cluster sizes and hence on the threshold criteria employed for delineating the functionally and anatomically defined areas. Apart from the area-based comparison, the probability for a specific functional voxel being located in an anatomically defined region was also calculated by reporting the aPM value at this coordinate and (in brackets) the range of aPM values for the surrounding voxels. Also, the weighted centres of gravity of functional and anatomical PMs were compared.

Finally, the applicability of the *hOc5* map for selecting functional imaging voxels for region-of-interest (ROI) analyses was tested. Bandpassed single-subject BOLD signal time courses (1/12–1/72 Hz) were averaged over fMRI voxels lying within the aPMs for *V1*, *V2*, and *hOc5*, respectively. Error bars indicate the standard deviations for BOLD signals of voxels within the respective ROI. Stereotactic coordinates are given in the anatomical MNI (aMNI) space, which has an origin that is 4 mm anterior and 5 mm ventral to the origin of the MNI space.

Results

All results presented here are based on the first half of each subject's data set (10 min recording time each), only. The second half of the data was not included in the analysis since after 10 min of fMRI measurement some subjects started to show signs of fatigue as could be observed via the eye movement control video camera. However, 10 min of data registration was sufficient to detect strong and reliable functional activations.

Dynamic versus stationary functional contrasts ($P_{\text{corr}} < 0.01$) showed bilateral activations of primary and secondary visual and the occipito-temporal cortical areas in all but subject 7036. However, subject 7036 exhibited similar activations at $P_{\text{corr}} < 0.05$. Figure 1 illustrates the aPMs' power in predicting these functional activations in individual subjects. Single subject functional t-maps (green, $P_{\text{corr}} < 0.01$, extent threshold of ten voxels) and aPMs (shades of grey) were both overlaid on transversal sections of the reference brain through the centre of gravity of the left *hOc5*.

For the group, significant bilateral activations were also seen in the predicted region of *V5/MT+* in the random-effects analysis (small-volume correction, see *Methods*). Figure 2 demonstrates the overlap of the functional group analysis t-maps (yellow) and aPMs (white). A quantitative comparison revealed that 19.0% (39.5%) of the right (left) functional activation was assigned to the right (left) *hOc5*. Conversely, 83.2% (53.5%) of the right (left) *hOc5* was functionally activated (Table 1, bottom). Centres of gravities for the small volume corrected activation clusters are given in Table 2 (second row). The centre of gravity of the

small-volume corrected cluster in the right *V5/MT+* (aMNI = [47, -73, 8]) was assigned to area *hOc5* with 40% probability (30–50%). The centre of gravity of the small-volume corrected cluster in the left *V5/MT+* (aMNI = [-44, -76, 10]) was assigned to area *hOc5* with 40% probability (20–40%).

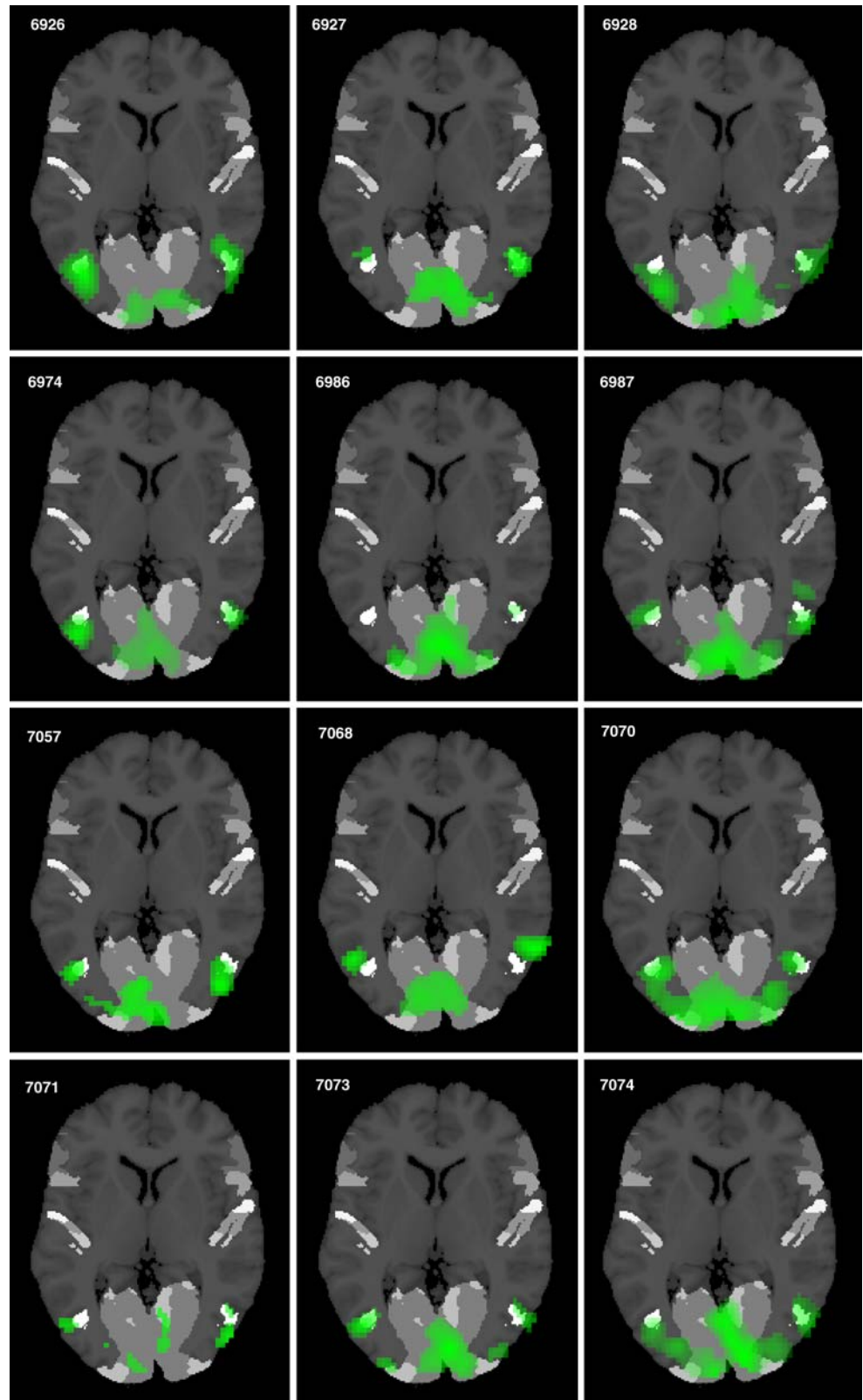
After a whole-brain instead of the small-volume correction for multiple comparisons (family-wise error rate $P_{\text{corr}} < 0.05$) the significantly activated area in the right occipito-temporal cortex shrank to 556 mm³ (blue outlined cluster in Fig. 2). The left group activation did not survive this threshold. A proportion of 65.8% of the remaining right occipito-temporal cluster was assigned to anatomically defined right *hOc5* and 47.9% of the right *hOc5* was functionally activated at this *t*-threshold (Table 1, bottom). The voxel with maximum *Z*-value in the right *V5/MT+* ($Z = 5.36$, aMNI = [51, -70, 11]) was assigned to *hOc5* with 40% probability (20–70%).

In a second approach, the fPMs were compared with their anatomical equivalents (Fig. 3). Quantitative data of brain volumes and percent-overlaps are given in Table 1. The right fPM had a volume of 2,267 mm³, 28.6% of which were assigned to anatomically defined right *hOc5*. In turn, most (84.9%) of the anatomically defined right *hOc5* was found to be functionally activated. The location of the right fPM's maximum was identical with the most significant voxel in the random effects group analysis (aMNI = [51, -70, 11]).

The left fPM had a smaller volume (1,528 mm³) than the right fPM. A proportion of 18.1% of the left fPM was assigned to the anatomical left *hOc5*. A fraction of 41.5% of the anatomically defined left *hOc5* was found to be functionally activated, that is, covered by the left fPM. The maximum of the left fPM (aMNI = [-48, -76, 17]) was assigned to anatomical *hOc5* with 30% probability (20–40%). Interestingly, the left PM volume was smaller than the right PM volume for both anatomical and functional data: the left aPM (622 mm³) was 87% of the size of the right aPM (719 mm³) and the left fPM (1,528 mm³) was 67% of the size of the right fPM (2,267 mm³). Figure 3 visualises the overlap between functional (red) and anatomical PMs (white). The centres of gravity for anatomical and functional PMs were similar as indicated by the superimposed cross-hairs in Fig. 3.

Figure 4 demonstrates the applicability of the aPMs for *hOc5* in selecting functional imaging voxels for ROI analyses. Bandpassed BOLD signal time courses (subject 6974, see *Methods*) were averaged over fMRI voxels lying within the aPMs for *V1*, *V2*, and *V5/MT+*, respectively. Obviously, the ROI defined by the aPMs for *hOc5* captures voxels that are strongly modulated by the alternating dynamic-stationary stimulation paradigm, that is, voxels that are motion-sensitive. However, a weaker stimulus-driven modulation of *V1/V2* ROIs is also visible and is the basis for the relatively strong *V1/V2* activation in the single-subject contrasts.

Fig. 1 Illustration of the predicting power of aPMs for functional activations in individual subjects. *Dynamic versus stationary* visual stimulation contrast (green $P_{\text{corr}} < 0.01$, extent threshold of ten voxels) and aPMs (shades of grey), both overlaid on transversal sections of the reference brain through the centre of gravity of the left *hOc5*. Inset numbers are subject identifiers. Subject 7036 exhibited no activations at this threshold, subject 7058 showed activations not seen in this section (both subjects not shown here)

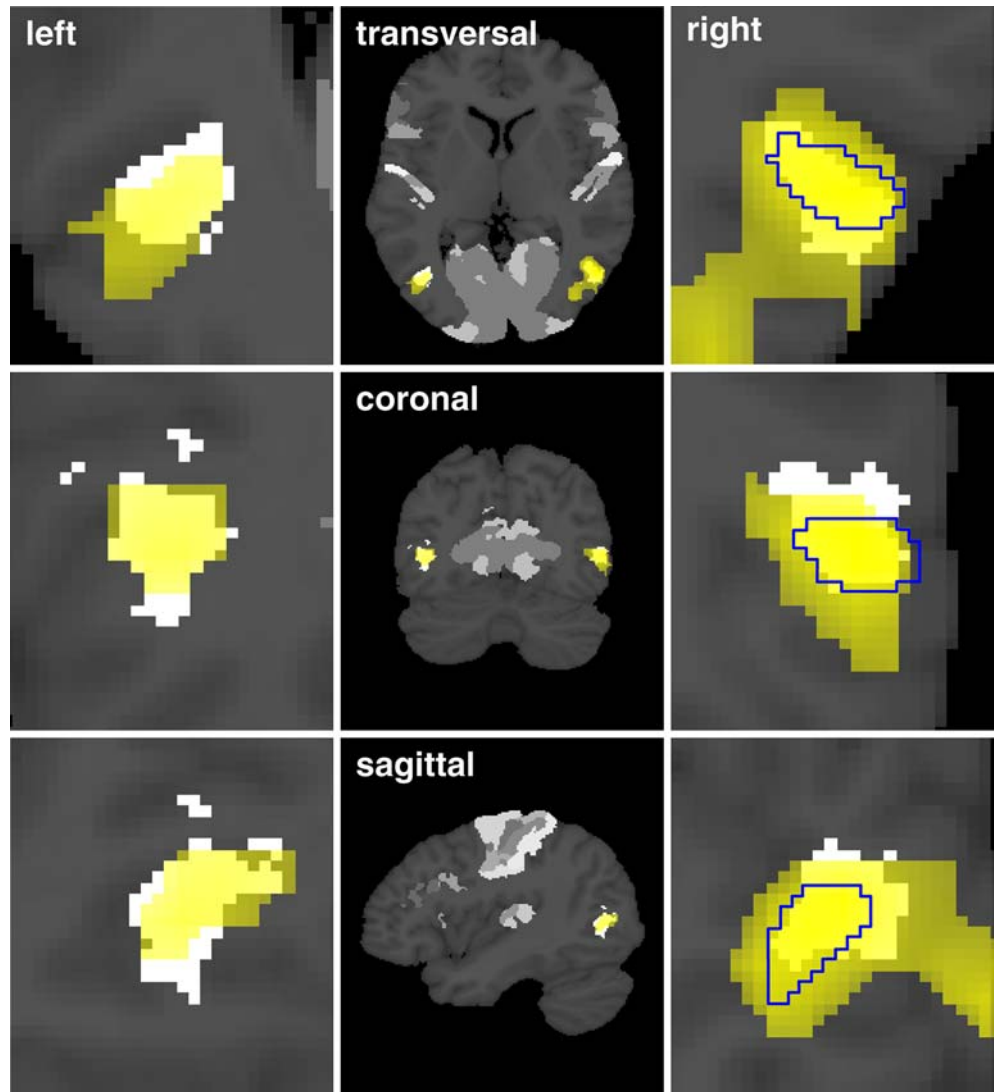


Discussion

We report here a functionally identified motion-sensitive visual area and its anatomical correlate as derived from

microscopic cytoarchitectonic studies of post-mortem brains. A comparison was made of the functionally and anatomically defined areas and a significant spatial overlap was found to exist.

Fig. 2 Overlap of functional group analysis t -maps (yellow small-volume correction, blue outline whole-brain correction) and anatomical PMs (white). Close-ups (left column) and whole-brain views (middle column) of the $V5/MT+$ region at the coordinates of the centre of gravity of the anatomical left $hOc5$ (aMNI = $[-43, -73, 10]$). Right column Close-ups of the $V5/MT+$ region at the coordinates of the centre of gravity of the anatomical right $hOc5$ (aMNI = $[49, -70, 11]$)



Functional activation in the dynamic versus stationary contrast

In addition to bilateral $V5/MT+$, visual areas $V1$ and $V2$ were more active during dynamic than during stationary stimulus presentation (Fig. 1). This is not surprising given that the stationary visual stimulus was more or less stabilised on the retina due to the fixation task. Such stimuli tend to fade away as the quick eye-movements that otherwise constantly refresh the input to the visual system are diminished or absent (Yarbus 1967). Contrary to that, dynamic stimuli bear potentially more information, thus recruit more neurons, and thus should produce a stronger BOLD signal. An alternative explanation for augmented neural activity in $V1$ and $V2$ during visual motion processing is provided by studies showing a *top-down* enhancement of neural activity in early visual processing areas (Fink et al. 1996; Kastner et al. 1998): it is indeed possible that the motion stimuli captured more attention than the stationary

stimuli resulting in increased *top-down* modulation of the neural processes underlying motion processing.

Significant random-effects group activations were found in the right but not the left $V5/MT+$ when a whole-brain correction for multiple comparisons was performed ($P_{\text{corr}} < 0.05$, Figure 2). However, using data from other fMRI and PET studies concerned with area $V5/MT+$ (Table 2) we were able to confirm bilateral activation of area $V5/MT+$ at a t -threshold corrected for the respective small volumes (spheres of 15 mm radius, see Methods). Nonetheless, activation clusters were greater in the right hemisphere than in the left hemisphere (Fig. 2). This asymmetry can be explained in several ways: first, stronger right-hemispheric activation in single subjects could amount to larger clusters of significant voxels. However, the most significant $V5/MT+$ voxels were as often found in the left as in the right hemispheres (Table 3), which leaves this explanation inconclusive. Second, greater inter-subject variability of the $V5/MT+$ activation clusters in the left

Table 1 Top: quantitative comparison of the overlap of functional and anatomical PMs for left, right, and summed bilateral *V5/MT+*. Given are the volumes of the functional PMs (columns 2, 5, and 8), the fraction of fPMs that were assigned to the respective left or right area *hOc5* (columns 3 and 6), and the fraction of *hOc5* that

was covered by the respective fPMs (columns 4 and 7). Bottom: comparison of the cluster volumes and percent overlap with area *hOc5* for fPMs, small-volume corrected random-effects analysis data (*rfx(svc)*), and the random-effects data corrected for multiple comparisons in the whole brain (*rfx*)

Functional PMs	Left <i>V5/MT+</i>			Right <i>V5/MT+</i>			<i>V5/MT+</i>
	Volume (mm ³)	% of fPM assigned to <i>hOc5</i>	% of <i>hOc5</i> covered by fPM	Volume (mm ³)	% of fPM assigned to <i>hOc5</i>	% of <i>hOc5</i> covered by fPM	Volume (mm ³)
70	5	20.0	0.1	2	50.0	0.1	7
60	188	11.7	3.3	205	84.4	22.6	393
50	658	18.8	18.6	1067	45.3	63.2	1725
40	1528	18.1	41.5	2267	28.6	84.9	3795

Map comparisons	Left <i>V5/MT+</i>			Right <i>V5/MT+</i>			
	Volume (mm ³)	% of map assigned to <i>hOc5</i>	% of <i>hOc5</i> covered by map	Volume (mm ³)	% of map assigned to <i>hOc5</i>	% of <i>hOc5</i> covered by map	
<i>fPM</i>	40%	1528	18.1	41.5	2267	28.6	84.9
<i>rfx(svc)</i>	$P_{\text{corr}} < 0.05$	903	39.5	53.5	3356	19.0	83.2
<i>rfx</i>	$P_{\text{corr}} < 0.05$	0	–	–	556	65.8	47.9
<i>aPM</i>	40%	622	–	–	719	–	–

than in the right hemispheres could result in a reduced overlap of activation clusters in the left compared with the right hemisphere. As an estimate for the inter-subject variability, we calculated the Euclidean distance between each subject's most significant voxel in *V5/MT+* and the mean location of the most significant voxel of all subjects (Table 2, third row and Table 3). Distances were 9.5 ± 7.6 mm and 8.7 ± 3.9 mm (mean \pm standard deviation) for the left and right *V5/MT+*, respectively. Thus, inter-subject variability was more pronounced in the left *V5/MT+*, but did not differ significantly between the hemispheres. Given that single subject left *V5/MT+* activations were neither weaker in terms of peak *t*-values (Table 3) nor more variant in their localization between subjects we would like to suggest that *V5/MT+* activations were physiologically spatially more confined to the left than the right hemisphere. In fact, as shown by the analysis of the fPMs, the left functional *V5/MT+* was about 67% of the size of the right functional *V5/MT+* (Table 1).

The greater confinement of the left *V5/MT+* activation could be based on the well-established right hemispheric dominance for visual attention (Heilman and Van den Abell 1980; Marshall and Fink 2001). According to Heilman and Van den Abell, the left hemisphere attends to contralateral stimuli whereas the right hemisphere attends to contralateral and ipsilateral stimuli. Thus, in healthy volunteers fullfield stimuli should provide stronger input to the right than to the left hemisphere and may thus lead to larger right hemispheric activations. This line of argument is supported by the observation of marked structural asymmetries between the hemispheres (Toga and Thompson 2003) and the occipital lobe in particular (Amunts et al. 2000;

Zilles et al. 1996). A right hemispheric predominance of *V5/MT+* activation has also been reported by Dupont et al. (1993, 1994), while others have not been able to observe differences between left and right hemispheric *V5/MT+* activations (Dumoulin et al. 2000).

Functional PMs

The centres of gravities for the small-volume corrected group activation clusters were similar to those of the functional and anatomical PMs (Table 2, second row). The small deviation of the right centre of gravity can be explained by a postero-medial cluster extension at this *t*-threshold (Fig. 2).

The use of functional PMs enabled us to compare similar approaches to data analysis (probability maps) rather than statistical *t*-maps versus probability maps. Interestingly, the left PM volume was smaller than the right PM volume for both, anatomical and functional data (87% and 67%, respectively), suggesting that fPMs and aPMs are indeed comparable measures for the same cortical entity.

A substantial overlap of fPMs and aPMs was observed: 28.6% of the right fPM was assigned to the corresponding right aPM and 84.9% of the right aPM was found to be functionally activated, that is, overlapped with the right fPM. Likewise, in the left hemisphere 18.1% of the left fPM was assigned to the corresponding left aPM and 41.5% of the left aPM was found to be functionally activated (Fig. 3). We suggest that the lesser degree of overlap in the left *V5/MT+* may at least in part be due to the more confined left *V5/MT+* activations as pointed out previously.

Table 2 *V5/MT+* coordinates in this study in comparison with other studies (*cog* centre of gravity; *hs* hemispheres; *normal fonts* reported original data, *italics* data transformed from/to Talairach/

aMNI space based on the script by (Brett 2002)). Coordinates are given in Talairach coordinates (*middle columns*) and aMNI coordinates (*rightmost columns*)

	<i>n</i>	<i>cog_{left}</i> (Tal)	<i>cog_{right}</i> (Tal)	<i>cog_{left}</i> (aMNI)	<i>cog_{right}</i> (aMNI)
Functional PM (<i>cog</i>) (40% maps)	14	<i>[-45, -69, 12]</i>	<i>[50, -66, 8]</i>	[-45, -76, 14]	[51, -72, 10]
Functional group RFX (<i>cog</i>) (small volume corrected)	14	<i>[-44, -70, 8]</i>	<i>[47, -67, 6]</i>	[-44, -76, 10]	[47, -73, 8]
Mean location of the most significant fMRI voxel	14	<i>[-45, -68, 12]</i>	<i>[51, -66, 8]</i>	[-45, -75, 14]	[52, -72, 10]
Anatomical PM (<i>cog</i>) (40% maps)	10	<i>[-43, -67, 8]</i>	<i>[49, -64, 9]</i>	[-43, -73, 10]	[49, -70, 11]
Dukelow et al. (2001)	5	-	[44, -66, 2]	-	<i>[44, -72, 3]</i>
Rees et al. (2000)	4	[-44, -64, -2]	[50, -66, 0]	<i>[-44, -70, -1]</i>	<i>[51, -72, 1]</i>
Dumoulin et al. (2000)	10, 9	[-47, -76, 2]	[44, -67, 0]	<i>[-47, -82, 3]</i>	<i>[44, -73, 1]</i>
Sunaert et al. (1999)	12 <i>hs</i>	[-42, -66, 2]	[42, -62, 6]	<i>[-42, -72, 3]</i>	<i>[42, -68, 8]</i>
Goebel et al. (1998)	5	[-48, -60, 2]	[45, -57, 5]	<i>[-48, -66, 4]</i>	<i>[45, -63, 7]</i>
Hasnain et al. (1998) (PET)	11	[-39, -72, -1]	[41, -65, 2]	<i>[-39, -78, 0]</i>	<i>[42, -71, 3]</i>
Smith et al. (1998)	15 <i>hs</i>	[-46, -70, 4]	[46, -70, 4]	<i>[-46, -76, 6]</i>	<i>[46, -76, 6]</i>
Beauchamp et al. (1997)	8	[-42, -70, 3]	[42, -70, 3]	<i>[-42, -76, 4]</i>	<i>[42, -76, 4]</i>
Dupont et al. (1997)	10	[-40, -70, -4]	[40, -64, 4]	<i>[-40, -76, -4]</i>	<i>[40, -70, 6]</i>
Tootell et al. (1995)	6	[-45, -76, 3]	[45, -76, 3]	<i>[-45, -82, 4]</i>	<i>[45, -82, 4]</i>
Dupont et al. (1994) (PET)	14	[-46, -72, 0]	[32, -74, 8]	<i>[-46, -78, 1]</i>	<i>[32, -81, 10]</i>
Watson et al. (1993) (PET)	12	<i>[-44, -70, 0]</i>	<i>[40, -68, 0]</i>	<i>[-44, -76, 1]</i>	<i>[40, -74, 1]</i>
Mean location in literature (i.e., a priori knowledge of <i>V5/MT+</i> location)		[-44, -70, 1]	[43, -67, 3]	[-44 -76 2]	[43 -73 5]

How does the location of *V5/MT+* fPMs relate to the literature data?

The mean location of the right *V5/MT+* in 12 functional studies listed in Table 2 (aMNI = [43, -73, 5]) was 10 mm away from the centre of gravity of the right fPM reported in this study (aMNI = [51, -72, 10]). The mean location of the left *V5/MT+* in the same studies (aMNI = [-44, -76, 2], N = 11) was 12 mm away from the centre of gravity of the left fPM in our data (aMNI = [-45, -76, 14]). The differences between the literature data and the results presented here are likely to result from inaccuracies produced by the transformation of coordinates between the different reference coordinate systems used in the respective studies. Most of the data listed in the literature on the locations of *V5/MT+* are presented in Talairach space (Talairach and Tournoux 1988). Calculations of Talairach from aMNI coordinates and vice versa are based on affine or non-linear

transformations that are inherently problematic and erroneous (Brett 2002). In contrast to that, the *V5/MT+* coordinates from our functional and anatomical data match very well since the coordinates of the functionally and anatomically delineated areas were compared in the same native aMNI space.

In conclusion, random-effects data as well as fPMs yield similar results. Due to the method of their generation, fPMs more closely resemble the aPMs. The convergence of both data modalities shows that the functionally defined human *V5/MT+* correlates with the cytoarchitectonic area *hOc5* obtained from post-mortem brains. This suggests that aPMs for *hOc5* can be employed to characterise functional activations of the motion-sensitive area *V5/MT+* in group analyses. However, due to the substantial inter-subject variability in the location of area *V5/MT+*, functional data is recommended for the localisation of *V5/MT+* in the individual brain.

Table 3 Inter-subject variability. Coordinates of the most significant voxels in *V5/MT+* for every subject contributing to this study. Bold *t*-values indicate whether the left or right hemisphere had the most significant voxel in *V5/MT+* in a particular subject.

Mean coordinates of most significant voxels for the left and right hemispheres as well as the mean distances to the respective mean coordinates are given in the *bottom rows*

Subject	Left (aMNI)	t_{left}	Right (aMNI)	t_{right}
6926	[-42, -76, 14]	16.19	[51, -73, 14]	14.71
6927	[-45, -64, 17]	8.39	[51, -73, 11]	10.34
6928	[-39, -88, 8]	15.79	[57, -76, 5]	14.05
6974	[-45, -82, 14]	19.75	[51, -73, 20]	17.00
6986	[-48, -79, 2]	8.78	[48, -70, 5]	9.49
6987	[-48, -73, 11]	13.10	[51, -58, 11]	9.21
7036	[-45, -76, 14]	6.03	[57, -76, 5]	7.86
7057	[-48, -76, 14]	10.14	[42, -82, 14]	10.54
7058	[-39, -88, 17]	7.49	[51, -73, 20]	7.66
7068	[-51, -67, 17]	13.27	[60, -61, 11]	13.47
7070	[-42, -46, 23]	8.38	[45, -73, 2]	14.42
7071	[-51, -76, 14]	8.08	[54, -73, 2]	9.38
7073	[-45, -76, 11]	12.57	[57, -76, 8]	8.85
7074	[-42, -79, 20]	14.87	[54, -76, 11]	11.77
Mean	[-45, -75, 14]	$n_{\text{max}} = 6$	[52, -72, 10]	$n_{\text{max}} = 8$
Mean distance to mean location	9.5 ± 7.6 mm		8.7 ± 3.9 mm	

Fig. 3 Overlap of functional (red) and anatomical (white) PMs. Close-ups (*left column*) and whole-brain views (*middle column*) of the *V5/MT+* PMs at the coordinates of the centre of gravity of the anatomical left *hOc5* (aMNI = [-43, -73, 10]). *Right column* close-ups of the *V5/MT+* PMs at the coordinates of the centre of gravity of the anatomical right *hOc5* (aMNI = [49, -70, 11]). *Cross-hairs* mark the centres of gravity of the aPMs (black) and fPMs (dark red)

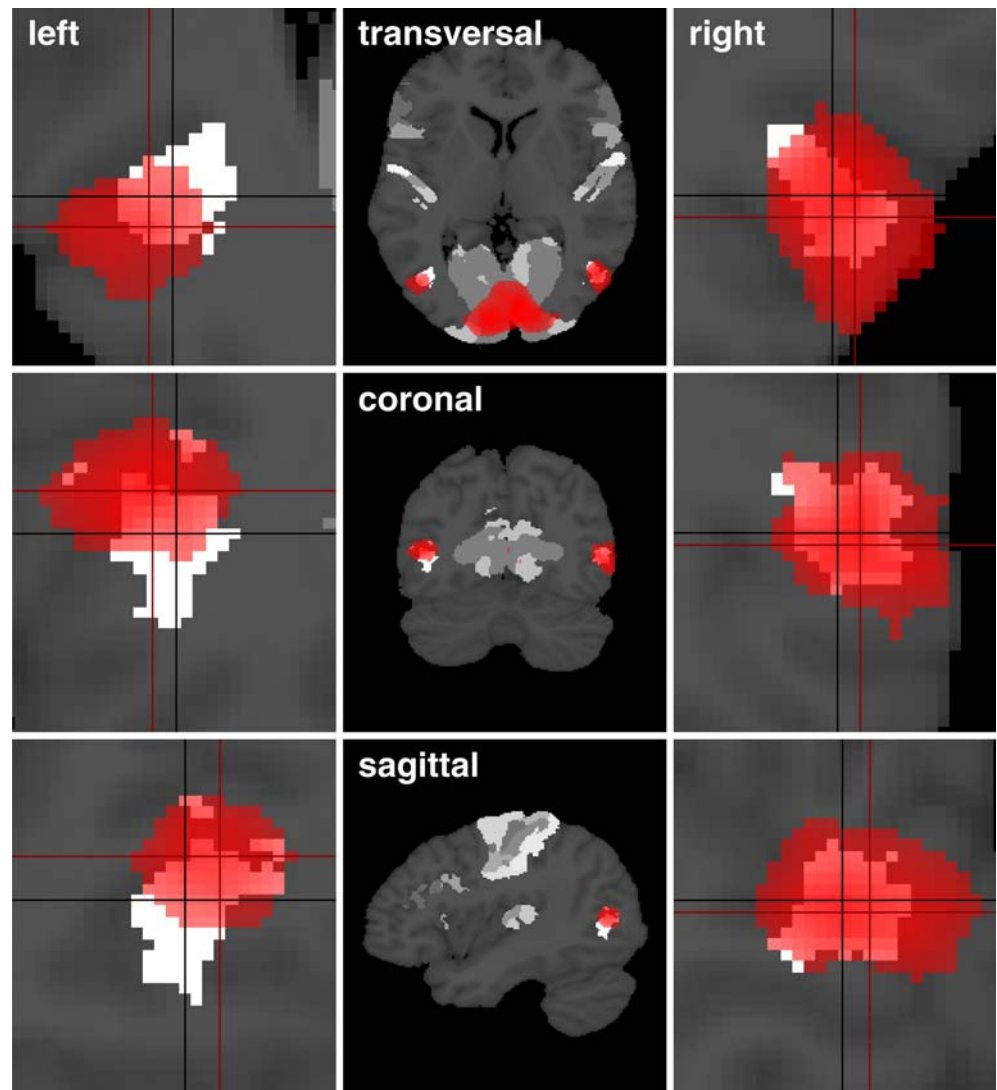
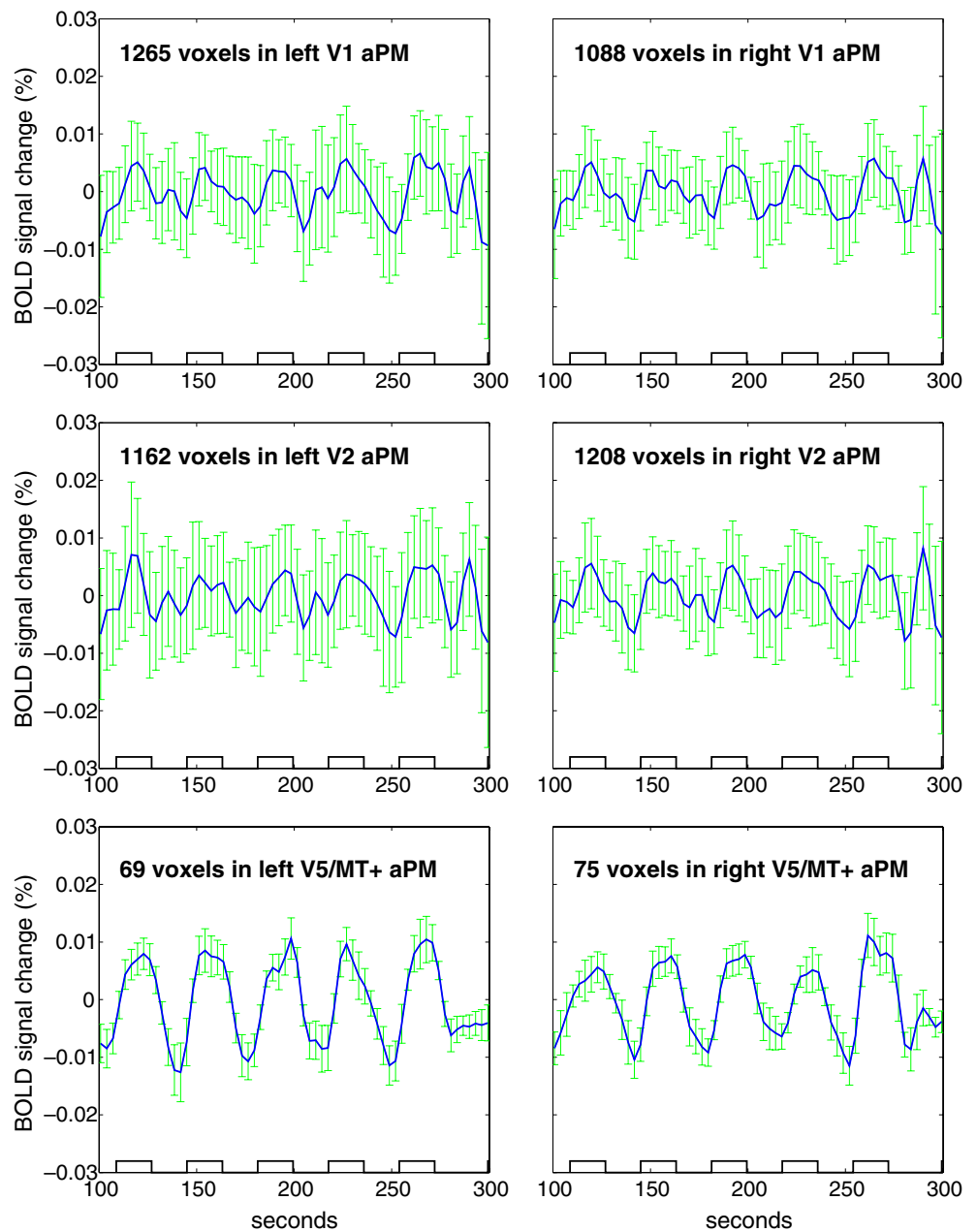


Fig. 4 Averaged BOLD signal time courses of fMRI voxels lying within the aPMs for *V1*, *V2*, and *V5/MT+* (from top to bottom, subject 6974). Boxes above the x-axes indicate dynamic visual stimulation periods



Acknowledgements We are grateful to our colleagues from the MR and Cognitive Neurology group for their assistance. Gereon R. Fink is supported by the Deutsche Forschungsgemeinschaft (DFG KPO-112, TP1 and TP8).

References

- Allman JM, Kaas JH (1971) A representation of the visual field in the caudal third of the middle temporal gyrus of the owl monkey (*Aotus trivirgatus*). *Brain Res* 31(1):85–105
- Amunts K, Malikovic A, Mohlberg H, Schormann T, Zilles K (2000) Brodman's areas 17 and 18 brought into stereotaxic space. Where and how variable? *NeuroImage* 11:66–84
- Annese J, Gazzaniga MS, Toga AW (2005) Localization of the human cortical visual area MT based on computer aided histological analysis. *Cerebral Cortex* 15(7):1044–1053
- Beauchamp MS, Cox RW, DeYoe EA (1997) Graded effects of spatial and featural attention on human area MT and associated motion processing areas. *J Neurophysiol* 78:516–520
- Brett M (2002) <http://www.mrc-cbu.cam.ac.uk/Imaging/Common/mnispaces.html>
- Collins DL, Neelin P, Peters TM, Evans AC (1994) Automatic 3D intersubject registration of MR volumetric data in standardized Talairach space. *J Comput Assist Tomogr* 18(2):192–205
- Dukelow SP, De Souza JFX, Culham JC, van den Berg AV, Menon RS, Vilis T (2001) Distinguishing subregions of human MT+ complex using visual field and pursuit eye movements. *J Neurophysiol* 86:1991–2000
- Dumoulin SO, Bittar RG, Kabani NJ, Baker CL Jr, Le Goualher G, Pike GB, Evans AC (2000) A new anatomical landmark for reliable identification of human area V5/MT: a quantitative analysis of sulcal patterning. *Cereb Cortex* 10:454–463
- Dupont P, Orban GA, Vogels R, Bormans G, Nuyts J, Schiepers C, De Roo M, Mortelmans L (1993) Different perceptual tasks

- performed with the same visual stimulus attribute activate different regions of the human brain: a positron emission tomography study. *PNAS* 90:10927–10931
- Dupont P, Orban GA, de Bruyn B, Verbruggen A, Mortelmans L (1994) Many areas in the human brain respond to visual motion. *J Neurophysiol* 72:1420–1424
- Dupont P, de Bruyn B, Vandenberghe R, Rosier A-M, Michiels J, Marchal G, Mortelmans L, Orban GA (1997) The kinetic occipital region in human visual cortex. *Cereb Cortex* 7:283–292
- Eickhoff SB, Stephan KE, Mohlberg H, Grefkes C, Fink GR, Amunts K, Zilles K (2005) A new SPM toolbox for combining probabilistic cytoarchitectonic maps and functional imaging data. *NeuroImage* 25:1325–1335
- Evans AC, Marrett S, Neelin P, Collins L, Worsley K, Dai W, Milot S, Meyer E, Bub D (1992) Anatomical mapping of functional activation in stereotactic coordinate space. *NeuroImage* 1:43–53
- Fink GR, Halligan PW, Marshall JC, Frith CD, Frackowiak RS, Dolan RJ (1996) Where in the brain does visual attention select the forest and the trees? *Nature* 382:626–628
- Flechsig P (1927) *Meine myelogenetische Hirnlehre mit biographischer Einleitung*. Springer, Berlin
- Friston KJ, Holmes A, Poline J-B, Price CJ, Frith CD (1996) Detecting activations in PET and fMRI: Levels of inference and power. *NeuroImage* 4:223–235
- Goebel R, Khorrarn-Sefat D, Muckli L, Hacker H, Singer W (1998) The constructive nature of vision: direct evidence from fMRI studies of apparent motion and motion imagery. *Eur J Neurosci* 10:1563–1573
- Hasnain MK, Fox PT, Woldorff MG (1998) Intersubject variability of functional areas in the human visual cortex. *Hum Brain Map* 6:301–315
- Heilman KM, Van den Abell T (1980) Right hemisphere dominance for attention: The mechanism underlying hemispheric asymmetries of inattention (neglect). *Neurology* 30:327–330
- Holmes CJ, Hoge R, Collins L, Woods R, Toga AW, Evans AC (1998) Enhancement of MR images using registration for signal averaging. *J Comput Assist Tomogr* 22:324–333
- Huk AC, Dougherty RF, Heeger DJ (2002) Retinotopy and functional subdivision of human areas MT and MST. *J Neurosci* 22:7195–7205
- Kastner S, De Weerd P, Desimone R, Ungerleider LG (1998) Mechanisms of directed attention in the human extrastriate cortex as revealed by functional MRI. *Science* 282:108–111
- Malikovic A, Amunts K, Schleicher A, Mohlberg H, Palomero-Gallagher N, Schormann T, Zilles K (2001) Cytoarchitecture and stereotactic location of a preoccipital area in the region of V5/MT. *NeuroImage* 13:S909
- Marshall JC, Fink GR (2001) Spatial cognition: where we were and where we are. *NeuroImage* 14:2–7
- Maunsell JHR, Nealey TA, DePriest DD (1990) Magnocellular and parvocellular contributions to responses in the middle temporal visual area (MT) of the macaque monkey. *J Neurosci* 10:3323–3334
- Mugler JP 3rd, Brookeman JR (1990) Three-dimensional magnetization-prepared rapid gradient-echo imaging (3D MP RAGE). *Magn Reson Med* 15(1):152–157
- O'Craven KM, Rosen BR, Kwong KK, Treisman A, Savoy RL (1997) Voluntary attention modulates fMRI activity in human MT-MST. *Neuron* 18:591–598
- Oldfield RC (1971) The assessment and analysis of handedness: The Edinburgh inventory. *Neuropsychologia* 9:97–113
- Rees G, Friston K, Koch C (2000) A direct quantitative relationship between the functional properties of human and macaque V5. *Nature Neuroscience* 3(7):716–723
- Schleicher A, Amunts K, Geyer S, Morosan P, Zilles K (1999) Observer-independent method for microstructural parcellation of cerebral cortex. A quantitative approach to cytoarchitectonics. *NeuroImage* 9:165–177
- Smith AT, Greenlee MW, Singh KD, Kraemer FM, Hennig J (1998) The processing of first- and second-order motion in human visual cortex assessed by functional magnetic resonance imaging fMRI. *J Neurosci* 18:3816–3830
- Sunaert S, van Hecke P, Marchal G, Orban GA (1999) Motion-responsive regions of the human brain. *Exp Brain Res* 127:355–370
- Talairach J, Tournoux P (1988) *Co-planar stereotaxic atlas of the human brain: 3-dimensional proportional system—an approach to cerebral imaging*. Thieme, New York
- Toga AW, Thompson PM (2003) Mapping brain asymmetry. *Nat Rev Neurosci* 4:37–48
- Tootell RBH, Reppas JB, Kwong KK, Malach R, Born RT, Brady TJ, Rosen BR, Belliveau JW (1995) Functional analysis of human MT and related visual cortical areas using magnetic resonance imaging. *J Neurosci* 15(4):3215–3230
- Watson JDG, Myers R, Frackowiak RSJ, Hajnal JV, Woods RP, Mazziotta JC, Shipp S, Zeki S (1993) Area V5 of the human brain: evidence from a combined study using Positron Emission Tomography and Magnetic Resonance Imaging. *Cereb Cortex* 3:79–94
- Wohlschläger AM, Specht K, Lie C, Wohlschläger A, Bente K, Pietrzyk U, Stöcker T, Zilles K, Amunts K, Fink GR (2005) Linking retinotopic fMRI mapping and anatomical probability maps of human occipital areas V1 and V2. *NeuroImage* 26(1):73–82
- Yarbus AL (1967) *Eye movements and vision*. Plenum Press, New York
- Zeki S (1974) Functional organization of a visual area in the posterior bank of the superior temporal sulcus of the rhesus monkey. *J Physiol* 236:549–573
- Zeki S, Watson JDG, Lueck CJ, Friston KJ, Kennard C, Frackowiak RSJ (1991) A direct demonstration of functional specialization in human visual cortex. *J Neurosci* 11(3):641–649
- Zeki S (1993) *A Vision of the Brain*. Blackwell Scientific Publications, Oxford
- Zilles K, Dabringhaus A, Geyer S, Amunts K, Qu M, Schleicher A, Gilissen E, Schlaug G, Steinmetz H (1996) Structural asymmetries in the human forebrain and the forebrain of non-human primates and rats. *Neurosci Biobehav Rev* 20(4):593–605